On the Importance of Feature Descriptors for the Characterisation of Texture.

S.A. Karkanis, G. D. Magoulas, D. Iakovidis, D.E. Maroulis
University of Athens, Department of Informatics,
TYPA Builds., 15784 Athens, Greece
{sk,magoulas,dmarou}@di.uoa.gr

and

M. O. Schurr
Eberhard-Karls-University of Tuebingen, Section for Minimal Invasive Surgery,
Waldhoernlestrasse 22, D-72072 Tuebingen, Germany.
marc.schurr@uni-tuebingen.de

ABSTRACT
In this contribution is investigated the use of textural descriptors as descriptors for primitive textural information in medical images. A few approaches have been presented in the literature to the direction of the discrimination of texture in medical images compared with similar approaches used for texture recognition. In this paper we try to prove that texture exists in medical images and can be encoded using the proposed statistical based descriptors. We have selected four different methods for the estimation of such descriptors. These have been tested in various texture images and in endoscopic medical images, attempting this way to create the texture models possibly exist in the images. The texture spaces described by the corresponding vectors of the features are used as input to different multilayer perceptron type neural networks for the characterization of images from their texture content. An in depth experimental study has been conducted comparing textural feature extraction techniques on various images along with a novel discrete wavelet transform based methodology.

Keywords: *Texture analysis, cooccuurrence matrices, fractal dimension, wavelets*

1. INTRODUCTION

An important problem in the development of medical systems is the design of complex image mechanisms that will be capable to discriminate among the different regions. The estimation of image characteristics requires significant effort in order to depict an image in terms of a representation that best matches its information content.

Texture plays an important role for the characterisation of regions from digital images. It carries information about the micro-structure of the regions and the distribution of the grey levels within such regions. A scheme for the recognition based on the texture information should be capable of encoding the properties of the texture using a number of descriptors. These descriptors are usually represented by sets of statistical measures defining by this way the vectors to be used, consequently, for the recognition.

2. DESCRIPTION OF THE PROPOSED APPROACH

This paper deals with the design of image indices for the labeling of the corresponding regions in terms of their second order characteristics and, more specifically, texture. The proposed index design scheme is simple: an image is divided in rectangular regions of predefined dimensions and each one is labeled according to its textural content. The approach followed has two major processing stages. The first stage consists of all the processing that will be performed on an image to extract all the identifiable features.

We usually choose a family of texture attributes that account for the main spatial relations between

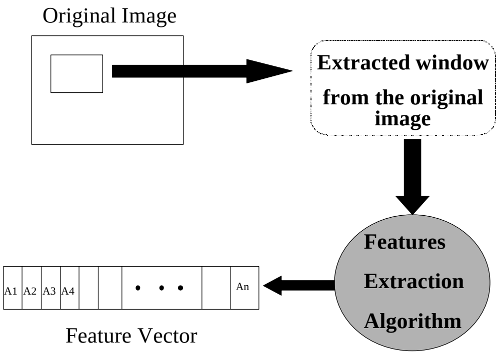

the grey levels of the texture. The image is divided in non-overlapping square regions of equal dimensions. The descriptors are estimated for each of these regions composing the textural feature vectors. These will then be used for the classification and labeling of these regions in terms of their textural content using statistical pattern recognition techniques.

In this paper we used statistical descriptors produced by three different transformations [1], [6-10]:

- Cooccurrence matrices
- Run length encoding
- Fractal dimension
- Discrete Wavelet Transform

The latter one is proposed as new descriptor for texture classification based on measures obtained from the detailed coefficients of the Discrete Wavelet Transform (DWT) [11-13]. An image division scheme into regions of square non-overlapping windows of equal dimensions has been adopted.
Multilayer Perceptron (MLP) type neural networks have been involved in the image classification and labelling approach of each window [3],[4].

3. FEATURE EXTRACTION

3.1 Cooccurrence matrices

Cooccurrence matrices [2] represent the spatial distribution and the dependence of the gray levels within a local area. Each (*i*,*j*)th entry of the matrices, represents the probability of going from one pixel with gray level (*i*) to another with a gray level (*j*) under a predefined distance and angle. From these matrices, sets of statistical measures are computed (called feature vectors) for building different texture models. In our experiments, we have considered four angles, namely 0, 45, 90, 135 as well as a predefined distance of one pixel in the formation of the cooccurrence matrices. Therefore, we have formed four cooccurrence matrices. According to our experiments, the following four statistical measures out of the 14, originally proposed by Haralick [2][3], provide high discrimination accuracy that can be only marginally increased by adding more measures in the feature vector:

- ***Energy - Angular Second Moment***

$$f_1 = \sum_i \sum_j p(i,j)^2$$

- ***Correlation***

$$f_2 = \frac{\sum_{i=1}^{N_g}\sum_{j=1}^{N_g}(i*j)\,p(i,j) - m_x m_y}{S_x S_y}$$

- ***Inverse Difference Moment***

$$f_3 = \sum_i \sum_j \frac{1}{1+(i-j)} p(i,j)$$

- ***Entropy***

$$f_4 = -\sum_i \sum_j p(i,j)\log\big(p(i,j)\big).$$

Thus, using the above mentioned four cooccurrence matrices we have obtained 16 features describing spatial distribution in each window

3.2 Run-length encoding

The run length matrix P with elements $p(i,j)$, where the (*i*)th dimension corresponds to the gray level and has a length equal to the maximum gray level *n*, while the (*j*)th dimension corresponds to the run length and has length equal to the maximum run length l, represents the frequency that (*j*) points with a gray level (*i*) continue in the direction *q* [12]. As with the cooccurrence matrix, $q = 0^{ï}$, $45^{ï}$, $90^{ï}$ and $135^{ï}$ offer the greatest interest. Five features can be calculated from the run length matrix as shown in the equations below:

- ***Long Run Emphasis***

$$r_1 = \frac{\sum_i \sum_j j^2 p(i,j)}{\sum_i \sum_j p(i,j)},$$

- ***Short Run Emphasis***

$$r_2 = \frac{\sum_i \sum_j \frac{p(i,j)}{j^2}}{\sum_i \sum_j p(i,j)},$$

- ***Gray Level Nonuniformity***

$$r_3 = \frac{\sum_i \left[\sum_j p(i,j)\right]^2}{\sum_i \sum_j p(i,j)},$$

- ***Run Length Nonuniformity***

$$r_4 = \frac{\sum_j \left[\sum_i p(i,j)\right]^2}{\sum_i \sum_j p(i,j)},$$

- ***Run Percentage***

$$r_5 = \frac{\sum_i \sum_j j^2 p(i,j)}{N^2},$$

where N^2 is the number of points in the image.

The run lengths are expected large for coarse textures, especially structural textures, but can be quite small for fine textures. The nonuniformity features are small if the gray levels or the run lengths are similar throughout the matrix, while the long run length is large if there is high intensity clustering in the texture.

3.3 Fractal dimension

The fractal dimension is a feature that characterizes the roughness of an image [8]. A well-known method for evaluating the fractal dimension is a variation of the well-known box-counting procedure, which is efficient and accurate for texture classification tasks [11].

Following this approach, the grey-level image is considered as a 3-dimensional space (x,y,z), with (x,y) denoting a 2-dimensional location, and (z) denoting the grey level. This 3-dimensional space is partitioned into cubes of size $r \times r \times r$. The position of the columns of the cubes, vertical to the (x,y) pixel plane is assigned as (i,j), where

$$(i,j) = (x/r, y/r),$$

and the boxes are enumerated from bottom to top. In every column (i,j) the cubes k and l which contain the minimum and maximum grey levels of the column, respectively, are found.

The fractal dimension D is estimated through the least mean square linear fit of $\log(N_r)$ against $\log(1/r)$ for different values of r:

$$D = \frac{\log(N_r)}{\log(1/r)}.$$

The number N_r is computed as

$$N_r = \sum_{i,j} n_r(i,j),$$

where $n_r(i,j) = l - k + 1$.

It is possible that two images of different texture and different optical appearance have the same fractal dimension. Thus, the discrimination capability of the fractal dimension, in some cases, is problematic. In order to alleviate this problem, the fractal dimension has been computed in the original subimage, as well as in the first two lower resolution versions of the original subimage and the first two sets of detail subimages, containing higher horizontal and vertical frequency spectral information. Decomposing the original image through the dyadic wavelet transform [6] has produced the subimages. The aforementioned feature extraction procedure is originally proposed in [4]. Following this procedure, seven-dimensional training patterns can be created from each image region.

3.4 DWT Textural Descriptor

The problem of texture discrimination, aiming at labeling image areas, is considered in the wavelet domain, since it has been demonstrated that discrete wavelet transform (DWT) can lead to better texture modeling [13]. We use the popular 2-D DWT schemes [6][14] performing a one-level wavelet decomposition of the image regions, thus resulting in four wavelet channels.

Concerning the wavelet decomposition of the image regions, among the one approximate and the three detail wavelet channels 2, 3, 4 (frequency index) we have selected for further processing only the three detail channels, whose variances are the largest, since they might carry more information than the approximate one. A more sophisticated approach is proposed by applying cooccurrence analysis to the three detail wavelet channels and extracting 3 16 = 48 relevant measures [13][14].

3.4.1 *Wavelet Transform*

Wavelets offer a general mathematical approach for hierarchical function decomposition. According to this transformation, a function, which can be a function representing an image, a curve, signal etc., can be described in terms of a coarse level in addition with details that range from broad to narrow scales. Wavelets offer an novel technique for computing the levels of detail present, under a framework that is based on a chain of *approximation* vector spaces $\{V_j \subset L^2(\Re^2),\ j \in Z\}$ and a *scaling* function f such that the set of functions $\left\{2^{-j/2} f\left(2^{-j} t - k\right): k \in Z\right\}$ forming an orthonormal basis for V_j. These two components introduce a mathematical framework presented by Mallat [6] and called multiresolution analysis.

A multiresolution analysis (MRA) scheme of $L^2(\Re^2)$ can be defined as a sequence of closed subspaces $\{V_j \subset L^2(\Re^2),\ j \in Z\}$ satisfying the following properties :

Containment : $V_j \subset V_{j-1} \subset L^2$; for all $j \in Z$.

Decrease: $\lim_{j \to \infty} V_j = 0$, i.e. $\bigcap_{j > N} V_j = \varnothing$, for all N

Increase : $\lim_{j \to -\infty} V_j = L^2$, i.e. $\bigcup_{j < N} V_j = L^2$, for all N.

Dilation : $u(2t) \in V_{(j-1)} \Leftrightarrow u(t) \in V_j$.

Generator : There is a function $f \in V_0$ whose translation $\{f(t - k : k \in Z)\}$ forms a basis for V_0 .

By defining *complementary subspaces* $W_j = V_{j-1} - V_j$ so that $V_{j-1} = V_j + W_j$ then we can write, according to the «*increase*» property that

$$L^2\left(\Re^2\right) = \sum_{j \in Z} W_j \qquad (1)$$

The subspaces W_j are called *wavelet subspaces* and contain the difference in signal information between the two spaces V_j and V_{j-1}. These sets contribute to a *wavelet decomposition* of L^2 according to Eq.(1).

4. DISCUSSION AND RESULTS

4.1 Texture Images

A total of 12 Brodatz texture images : 3, 5, 9, 12, 15, 20, 51, 68, 77, 78, 79, 93 (as shown in the following figure) of size 512×512 has been used. From each texture image 10 subimages of size 256×256, with 256 gray levels depth, were randomly selected, and the above mentioned feature extraction techniques have been applied. The MLP generalization capability has been tested using patterns from 20 subimages of the same size randomly selected from each image.

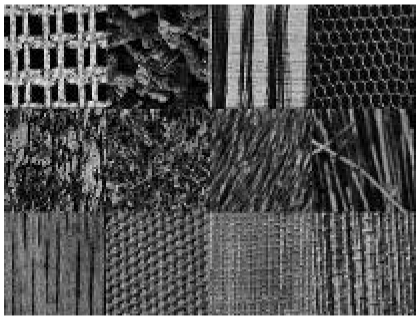

Figure 1. Twelve textures found in the "Brodatz Album".

A recently proposed learning algorithm, named BPVS, has been used to train the MLPs. For each feature extraction method thirty simulation runs have been performed using MLPs with 5 to 50 neurons in the hidden layer in order to find the architecture with the best average generalization capability. The best available architecture for each case is exhibited in Table 1. For example, a MPL with 48 input neurons, 30 hidden and 12 output neurons with biases exhibited the best performance for the DWT.

Feature extraction method	MLP
DWT distribution estimation	48-30-12
Fractal dimension	7-30-12
Cooccurrence analysis	16-40-12
Gray level run length moments	5-10-12

Table 1. The best available MLP architectures.

The average generalization performance of the 30 MLPs that have been trained using DWT features was the best and reached a 99.1%. The number of misclassified test patterns out of 240 for each method is presented in Figure 2. As shown in Figure 2, the MLPs that have been trained using the DWT distribution estimation patterns had significantly better generalization capability than all the others. For example, 13 MLPs trained with DWT distribution estimation patterns misclassified only 3 test patterns out of 240. On the other hand, 15 MLPs trained with Fractal dimension patterns misclassified 13 test patterns out of 240. Note that one MLP trained with DWT distribution estimation patterns achieved 100% classification success, i.e. it exhibited 0 misclassifications.

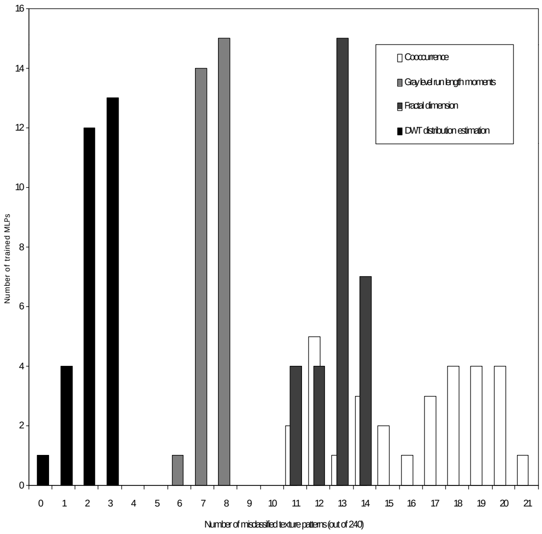

Figure 2. Number of trained MLPs with respect to corresponding misclassified test patterns.

4.2 Endoscopic Images

In the experiments reported a 16-21-2 MFNN architecture (i.e. 16 linear input neurons, 21 nonlinear hidden neurons and 2 nonlinear output neurons) has been used and the cooccurrence matrices for the textural description of tissue samples have been applied. Preliminary results have indicated that this scheme is capable of detecting abnormalities within the same colonoscopic image with 99% of success.

Below, we present results on detecting abnormalities, which belong to two different types, in colonoscopic images taken from two different colons. Image 1 (Fig. 3) is macroscopically a Type IIIs lesion according to (Kudo, 1996) [14]. Histologically it is a *low grade cancer*. Image 2 is macroscopically a Type V lesion according to (Kudo, 1996) [14]. Histologically it is a *moderately differentiated carcinoma*. In both cases the performance of the trained MFNNs has been tested on a set of 80 texture samples (40 normal and 40 abnormal) from the two images.

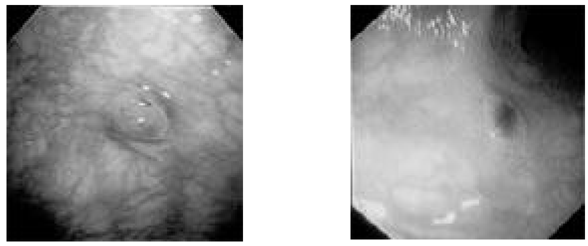

Image 1 Image 2

Figure 3. Colonoscopic images used

The average performance of 10 MFNNs than have been trained on this task is summarized in Table 2. The reported parameters are: CE is classification error in the training phase, m_{CS} is the average percentage of success in the testing phase and the computational cost required to train the networks is exhibited in terms of the average number of gradient (m_{GRD}) and of error function evaluations (m_{EFE}). Note that the value of the m_{CS} is very similar for the two cases, however the computational cost is quite different.

CE	m_{CS}	m_{GRD}	m_{EFE}
0.15	92.1	87	165
0.20	91.4	9	18

Table 2. Average performance of the 10 trained MFNNs.

Details on the generalization performance of the 10 networks are exhibited in Figure 4. Note, that MFNNs trained according to the first termination condition (CE<0.15) exhibit better performance than networks trained using the second condition. For example, one network trained using the condition CE<0.15 misclassified 3 out of the 80 test samples (i.e. success 95%), while two networks trained according to the condition CE<0.20 misclassified 5 out of the 80 test samples (i.e. success 93.75%).

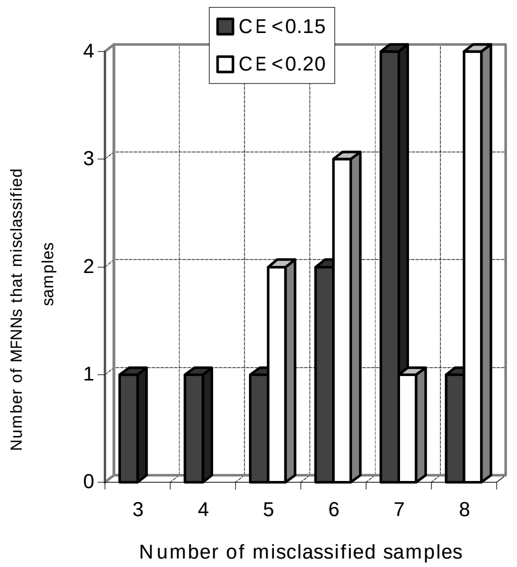

Figure 4. Number of trained MFNNs with respect to corresponding misclassified samples.

5. CONCLUSIONS

An image-indexing scheme for region-labeling applications based on image textural content has been proposed and preliminary evaluated. Regarding its components, a novel DWT distribution estimation technique has been suggested for the texture description stage. This method, along with three other well known feature extraction techniques, have been comparatively investigated in terms of their effects on the generalization performance of the labeling component of the indexing system. The preliminary results indicate that the proposed approach is considerably reliable for demanding applications.

6. REFERENCES

[1] Karkanis S, Magoulas GD, Grigoriadou M, Schurr M. Detecting abnormalities in colonoscopic images by textural description and neural networks. In: *Proc. of Work. on Mach. Learn. in Med. Appl., Advance Course in Artif. Intell.-ACAI99.* Chania: Greece, 1999: 59-62.

[2] Lim CP, Harrison RF, Kennedy RL. Application of autonomous neural network systems to medical pattern classification tasks. *Artificial Intelligence in Medicine* 1997; **11:** 215-239.

[3] Miller AS, Blott BH, Hames TK. Review of neural network applications in medical imaging and signal processing. *Medical and Biological Engineering and Computing* 1992; **30:** 449-464.

[4] Phee SJ, Ng WS, Chen IM, Seow-Choen F, Davies BL. Automation of colonoscopy part II: visual-control aspects. *IEEE Engineering in Medicine and Biology* May/June 1998: 81-88.

[5] Reategui EB, Campbell JA, Leao BF. Combining a neural network with case-based reasoning in a diagnostic system. *Artificial Intelligence in Medicine* 1996; **9:** 5-27.

[6] Gotlieb C.C., Kreyszig. Texture descriptors based on cooccurrence matrices. *Comp. Vision, Graph. and Image Proc.* 1990; **51:** 70-86.

[7] Haralick RM. Statistical and structural approaches to texture. *IEEE Proc.* 1979; **67:** 786-804.

[8] Galloway MM. Texture analysis using grey level run lengths. *Comp. Graph. and Image Proc.* 1975; **4:** 172-179.

[9] Weszka JS, Dyer CR, Rosenfeld A. A comparative study of texture measures for terrain classification. *IEEE Tr. Sys. Man and Cybernetics* 1976; **6:** 269-285.

[10] Chen CH. A study of texture classification using spectral features. In: *Proc. Int. Conf. Pattern Recognition*. Munich: Germany, 1982: 1074-1077.

[11] Cohen FS., Fan Z., Patel MA. Classification of rotated and scaled textured images using gaussian-markov random field models. *IEEE Tr. Pattern Anal. and Mach. Intelligence* 1991; **13:** 192-202.

[12] Kashyap RL, Chellappa R. Estimation and choice of neighbours in spatial interaction models of images. *IEEE Tansr. Information Theory* 1983; **29:** 60-72.

Durbin R, Miall C, Mitchison G. *The Computing Neuron.* Reading: Addison-Wesley, 1989.

[13] Kudo S. *Early Colorectal Cancer.* Tokyo: Igaku-Shoin Publischers, 1996.